WILEY | Hindawi

Research Article

Energetic and Exergetic Performance Investigation of Different Topologies for Hybrid Fuel Cell Vehicles

Ceyda Kök [1] **and Suha O. Mert** [2]

^{1}Department of Energy Systems Engineering, Institute of Graduate Studies, Iskenderun Technical University, 31200, Turkey
^{2}Department of Petroleum and Natural Gas Engineering, Iskenderun Technical University, 31200, Turkey

Correspondence should be addressed to Suha O. Mert; orcun.mert@iste.edu.tr

The use of green energy has increased day by day. Environmentally friendly hybrid electric vehicles with low CO_2 emissions have gained public attention. However, most battery electric vehicles are still having range problems, and emission values of hybrid electric vehicles are still not at the desired levels. Thus, fuel cell vehicles have gained some attention as good alternatives. The primary energy source for these vehicles is fuel cells, which are used in conjunction with batteries and supercapacitors to increase system performance. The combination of fuel cell + battery, fuel cell + supercapacitor, and fuel cell + battery + supercapacitor systems are currently the most popular topologies in this technology. The performance of these topologies is related to the overall energy efficiency and exergy efficiency of the vehicle model. Energy and exergy are two basic terminologies used to determine system performance and quality. Exergy determines the thermodynamic losses that cannot be determined using energy formulations alone. Thereby, it is very important to use both terminologies together to examine the performance of topologies and to determine any system losses. For this purpose, in this study, fuel cell + battery, fuel cell + supercapacitor, and fuel cell + battery + supercapacitor topologies were prepared and applied for Urban Dynamometer Driving Schedule (UDDS), Highway Fuel Economy Test Cycle (HWFET), New European Driving Cycle (NEDC), and Federal Test Procedure (FTP) driving cycles. Comparisons of these topologies in fuel consumption, power performance, and energy and exergy efficiencies were performed for the driving cycles. Also, energy flow, during the driving cycle, has showed and interpreted for the fuel cell vehicle that is designed and analyzed.

1. Introduction

Growing societies and developing technology result in increased energy demand, and when this demand is fulfilled using primarily fossil fuels, environmental pollution ensues. The use of fossil fuels results in the release of harmful gases like carbon dioxide and methane [1]. These are polluting gases, which are also known as greenhouse gases as they cause global warming.

Transportation is a major part of human civilization and unfortunately, it is also the part where the most amount of fossil fuels is consumed. Combustion engine vehicles release harmful emissions such as carbon dioxide (CO2), carbon monoxide (CO), and hydrocarbon (HC) [2]. These toxic gases threaten human health and nature. For this reason,

the orientation towards sustainable and clean energy sources is increasing with each passing day. Scientists and researchers have presented hybrid electric vehicles (HEA) and electric vehicles (EA) as a solution to this issue.

Hybrid electric (HE) vehicles consist of an electric motor and an internal combustion engine, representing a transition vehicle between today's internal combustion engine vehicles and future battery electric vehicles. A hybrid electric vehicle still uses fossil fuels such as gasoline and diesel. Although these vehicles have reduced greenhouse gas emissions, as of this study, they are still far from the target emission rates.

Electric vehicles (EVs), on the other hand, consist of one or more electric motors and some arrangement of batteries. These have zero emissions as they do not use fossil fuels. While the Lithium ion (Li-ion) batteries used in these

vehicles have many advantages—such as long shelf life, wide operating range, and high power and energy density—they also have certain disadvantages such as long charging times, low range, and limited charging possibilities.

As an alternative to HE and EV, the automotive industry has developed a new technology called fuel cell electric vehicles (FCEV), which can charge in a shorter time, have a longer range, and have zero emissions.

The energy carrier of FCEVs is hydrogen. Hydrogen is preferred in vehicle applications due to its small comparative volume while still having the highest content of fuel by weight. An FCEV feeds the electric motor with energy from the fuel cell. However, since the fuel cells have low energy density and approximately 60% efficiency, they cannot provide the fast starting and acceleration advantages of traditional internal combustion engine vehicles [3]. To solve this issue, fuel cells are integrated with batteries and supercapacitors in new FCEV vehicles [4]. By using fuel cells together with batteries and supercapacitors, the size of the fuel cell is reduced, which reduces the overall system weight as well. At the same time, with the additional energy provided by the battery and supercapacitor, hydrogen consumption is minimized, and the running costs are reduced. With such a dual energy system, the overall durability is also increased as the physical constraints of the fuel cells are reduced as well.

FCEVs are generally classified into three different topologies as fuel cell + battery, fuel cell + supercapacitor, and fuel cell + battery + supercapacitor vehicles. The fuel cell + battery configuration is a popular topology that meets the rapid acceleration expectations of internal combustion engine vehicle users by providing extra power to the fuel cell with the regenerative braking of the battery. Pioneering automobile brands such as Toyota, Honda, and Hyundai have started to produce vehicles that utilize fuel cell + battery hybrid systems [5]. The fuel cell + supercapacitor topology creates an ideal hybridization with the slow dynamics of the fuel cells and the high power density and fast response of a supercapacitor. In fuel cell + battery + supercapacitor topology, the battery and the supercapacitor work together to help the vehicle climb and accelerate. At the same time, thanks to the supercapacitor power density, the battery life is extended as the batteries require less charge/discharge.

In literature, many studies were performed on FCEV with different angles of approach. Optimization and cost analysis of fuel cell-based vehicles in FC + B, FC + SC, and FC + B + SC topologies were performed, and their performance were compared by Bauman et al. [5]. The importance of hybridization degree in FC + SC topology in vehicle performance and fuel economy has been examined by Feroldi et al., and fuel cells and supercapacitor hybridization were found to be performance-meaningful [6]. In the FC + B and FC + SC topologies, the performance comparison was made by changing the module numbers and vehicle weights of the energy storage systems. According to the results, when the number of battery modules in the FC + B Topology is increased, the fuel economy decreases while the performance increases. In FC + SC topology, fuel economy and performance increased when the number of modules is increases

[7]. Fuel cell-based hybrid vehicles require a complex control system as they are integrated with different power sources. How the power flow is divided between different sources and how the appropriate operating modes are determined depends on the energy management system (EMS). The main purpose of EMS is to share power between the powertrains by selecting the appropriate operating mode. It is also one of the objectives of ensuring the lowest fuel consumption, reducing emissions, and extending the lifetime of the components by selecting modes that meet their charging state capacities. There are various EMSs designed and optimized for hybrid control systems [8–11] in the literature. Linear programming and PID controller [12–14], state flow algorithms and multimode control [15–17], dynamic programming techniques [18], fuzzy logic control [19] model predictive control, and optimal control theory [20] are some of the applied strategies. Wu et al. aimed to increase battery efficiency and minimize hydrogen consumption with the ROEMS (robust energy management system) they applied to FC + B topology [21]. Wang et al. reduced fuel consumption by 21% and 36%, respectively, in two different driving cycles in the FC + SC topology [22]. Valdez-Resendiz et al. showed that they reduced energy waste by 14% by controlling the charge and discharge of the supercapacitor bank with the FLC (fuzzy logic control) energy management strategy in the FC + B + SC topology [23].

In fuel cell vehicles, besides energy efficiency, exergy efficiency is also very important. Energy and exergy are two interrelated terminologies that are used to measure the quality of a given system. Energy analysis cannot provide the real performance values of a system and cannot identify the factors that cause losses. However, exergy analysis does not have these shortcomings, and it can determine the actual performance of a given system while identifying the parts where losses occur.

In this study, fuel cell+battery, fuel cell+supercapacitor, and fuel cell+battery+supercapacitor topologies are modeled with the Matlab-ADVISOR program in order to compare important topologies of fuel cell vehicles. UDDS, HWFET, NEDC, and FTP driving cycles are applied to the modeled topologies. In addition to the energy efficiency of the entire system in each topology and in each driving cycle, exergy analysis was also performed, which shows the real performance value of the systems. Because of sustainability and exergy, which have a superior side of energy, exergy analysis is very important in this study. In addition, with fuel economy vehicle, performances in the driving cycles of the designed vehicles were compared. The power sharing between the energy storage systems in the three topologies is shown, and the energy flow in the optimal performing topology is examined.

2. Fuel Cell Hybrid Vehicles

Fuel cells convert the chemical energy in the fuel into electrical energy by electrochemical means. Since there is no combustion during this process, fuel cells only evacuate heat and water. Vehicles that use fuel cells as primary power sources are considered environmentally friendly, and many people
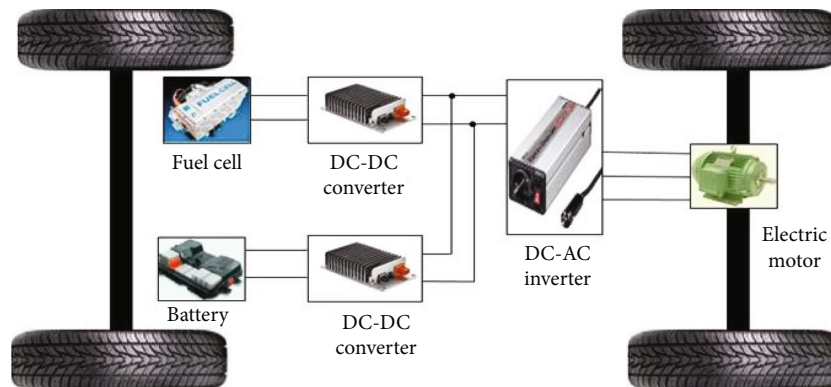
FIGURE 1: Fuel cell+ battery topology.

believe that they are the vehicles of the future since they do not use fossil fuels and have no harmful emissions [24].

Fuel cell vehicles are currently at the forefront as they have advantages such as short refueling time, long driving distances, and environmental safety. However, fuel cells cannot recover braking energy because they have a slow dynamic response [2]. They also cause gas starvation at fast power transitions. For this reason, batteries and supercapacitors are used in conjunction with fuel cells' compensation energy. The main purposes of using fuel cells with batteries and supercapacitors are to reduce fuel cell size, hydrogen consumption, and cost [4].

2.1. Fuel Cell + Battery Topology. With the increasing interest in fuel cell-based vehicles, these vehicles are expected to have a similar power density and fast start-up to today's internal combustion engine vehicles. Additional power required for this target is provided by connecting a battery to the fuel cell system. The battery contains regenerative braking energy, and it provides extra power based on the driver's acceleration demand, allowing the fuel cell to operate in its efficient region. Figure 1 shows the fuel cell battery topology.

2.2. Fuel Cell + Supercapacitor Topology. Supercapacitors are preferred in fuel cell vehicle applications because they are energy storage devices with a high power density and a short response time. The slow dynamics of the fuel cell and the fast response of the supercapacitor make an ideal duo and can efficiently meet the driver's power and speed demands. Figure 2 shows the fuel cell supercapacitor topology.

2.3. Fuel Cell+ Battery+ Supercapacitor Topology. In this topology, the demands for fast transient power, including acceleration, climbing, and braking of the vehicle, are covered by the supercapacitor. This ensures that the life of the battery is extended without being exposed to too much charge and discharge. By gaining braking energy, the supercapacitor relieves the load of the battery and fuel cell system with the highest power. Figure 3 shows the fuel cell, battery, and supercapacitor topology.

3. Materials and Method

3.1. ADVISOR- (Advanced Vehicle Simulator-)MATLAB. The Advanced Vehicle Simulator (ADVISOR) was programmed and developed by the US National Renewable Energy Laboratory (NREL) in the late 1990s. It was originally developed to support the US Department of Energy in the research of hybrid propulsion systems. ADVISOR is widely used by automobile manufacturers and university and institute researchers around the world. ADVISOR has a user-friendly interface and was built with Matlab/Simulink, the module of the Matlab program that can perform modeling, simulation, and analysis of dynamic systems. The program has been developed to support time-dependent and instantaneous, linear, and nonlinear systems and hybrid systems over time [6, 25].

3.2. Vehicle Models. Figure 4 shows the simulation block diagram of the fuel cell vehicle.

The block diagram in Figure 4 includes the driving cycle, fuel cell system, power bus, electric motor, gearbox, differential, energy storage system, wheels, and auxiliary systems. In this system, the speed demand of the driver or the driving cycle is transmitted to the wheel/axles, and the wheels convert the speed demand into torque. The torque demand is transmitted to the electric motor and transferred to the power bus for conversion to power demand. The power bus is the core of all vehicle control. The power bus receives power demand from each subsystem and the power capacity it can handle. In line with this information, it makes the sharing between power systems.

The primary power source of the designed vehicle is the fuel cell system. The fuel cell system first receives the signal of the power demanded by the electric motor and calculates the power that can be supplied by its system. The calculated power is transferred to the power bus. The power bus determines how much power it should demand from the energy storage system (battery or supercapacitor). The energy storage system calculates the power it will obtain with the signal it receives from the power bus and sends it to the power bus. The demanded power and the power from the energy storage systems are refed to the power bus.
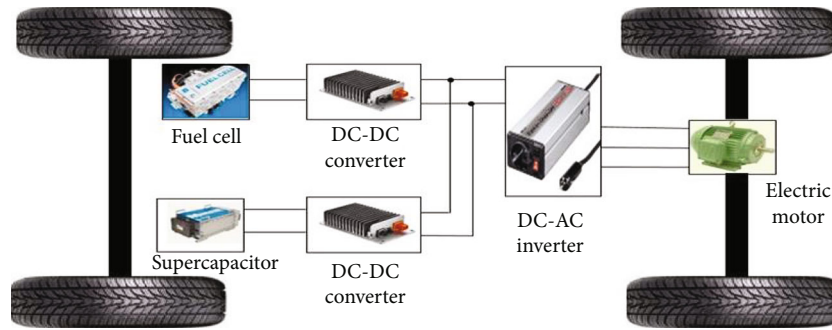
FIGURE 2: Fuel cell+ supercapacitor topology.
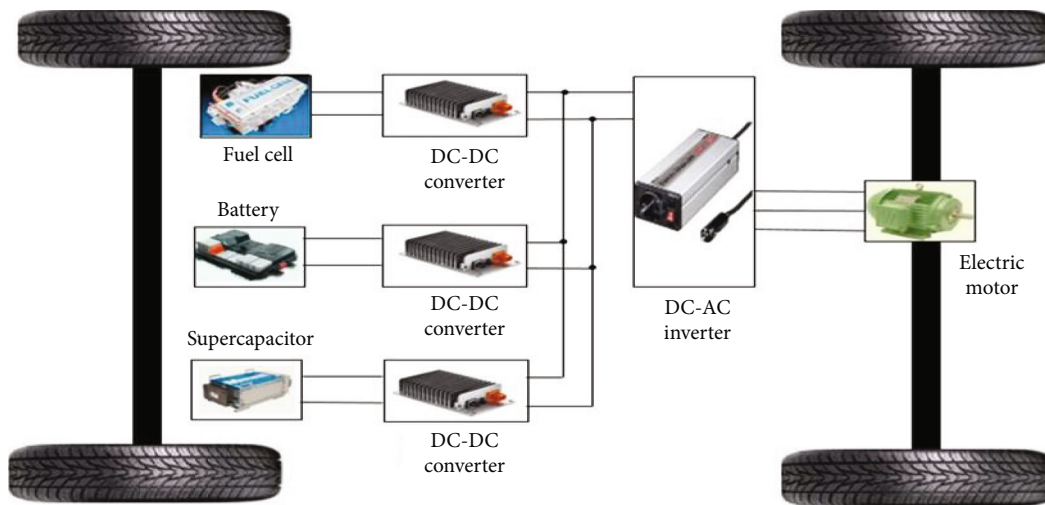
FIGURE 3: Fuel cell+battery+supercapacitor topology.
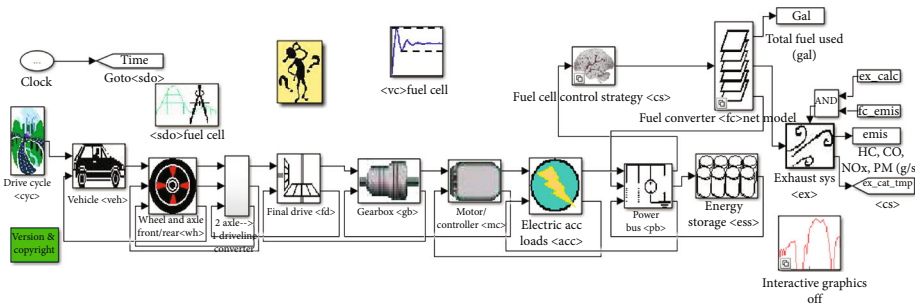
FIGURE 4: Fuel cell vehicle simulation block diagram.

In FC + B and FC + SC topologies, the fuel cell system determines whether to turn on according to the battery or supercapacitor state of charge and the power demanded. If the state of charge of the battery or supercapacitor is sufficient, it is expected that all power energy storage systems will be provided. If the state of charge is not sufficient, the fuel cell must provide all the power. If the state of charge is within the specified range, it is expected that the battery or supercapacitor will provide additional power to the fuel cell system.

In the FC + B + SC topology, in the power distribution strategy, fast power demands are required to be provided by the supercapacitor. Because if the vehicle performs regenerative braking when the battery charge state is close to full,

overcharging of the battery may occur and shorten the life of the battery. Taking advantage of the high power density feature of the supercapacitor, it is desired that the sudden power demands are provided by the supercapacitor. Therefore, the demand power of the supercapacitor on the power bus is set to 0. In this strategy, it is expected that the power demanded by the engine will be provided by the battery and supercapacitor in addition to the primary energy source fuel cell. When the demand power is greater than 0, it means that the energy storage system is discharged. In this case, if the charge state of the supercapacitor is not sufficient or the demand power is low, the battery assumes all the power. If the supercapacitor state of charge is sufficient, it provides
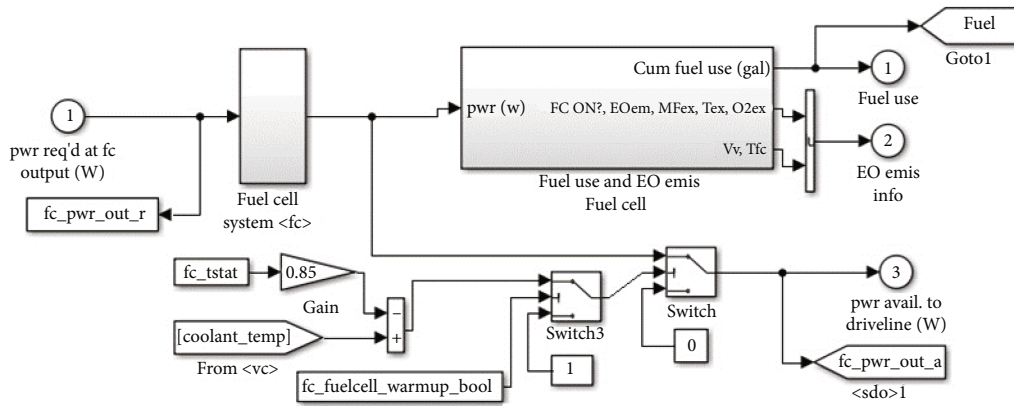
Figure 5: Fuel cell model.
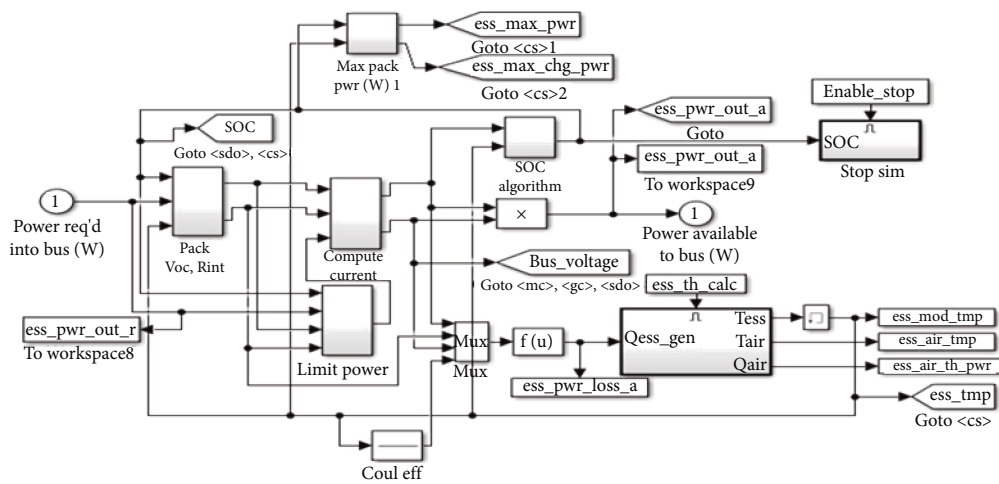
Figure 6: Battery model.
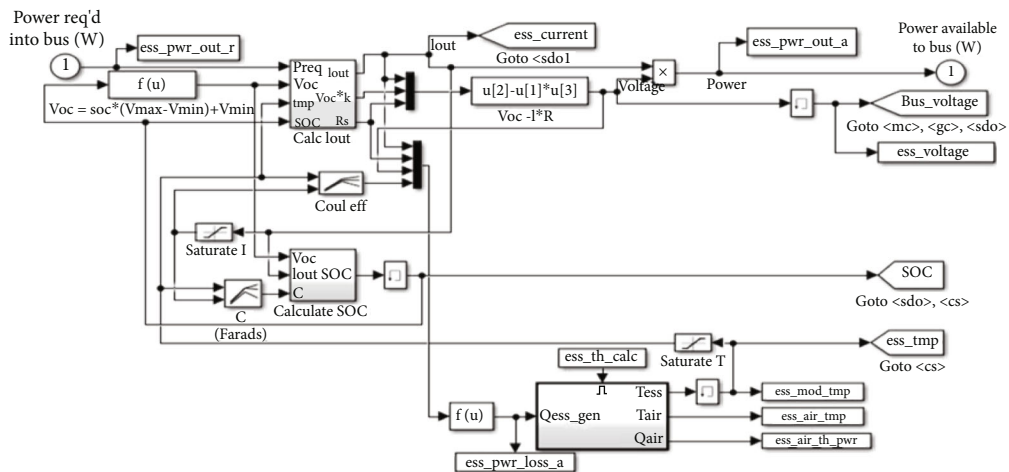
Figure 7: Supercapacitor model.

additional power to the battery. When the demand power is less than 0, it means that the energy storage system is charging. In this case, the supercapacitor starts charging the battery. If the supercapacitor is not at a sufficient charge level, the supercapacitor is charged first, and the battery is charged with the remaining power.

3.3. Fuel Cell Model. The fuel cell system modeled in the simulation program as part of this study is shown in Figure 5. The fuel cell system first receives the power signal according to the speed requested by the driver. According to the power signal, the lower block calculates the amount of fuel to be sent from the system. However, this fuel is

(a)

(b)

(c)

(d)
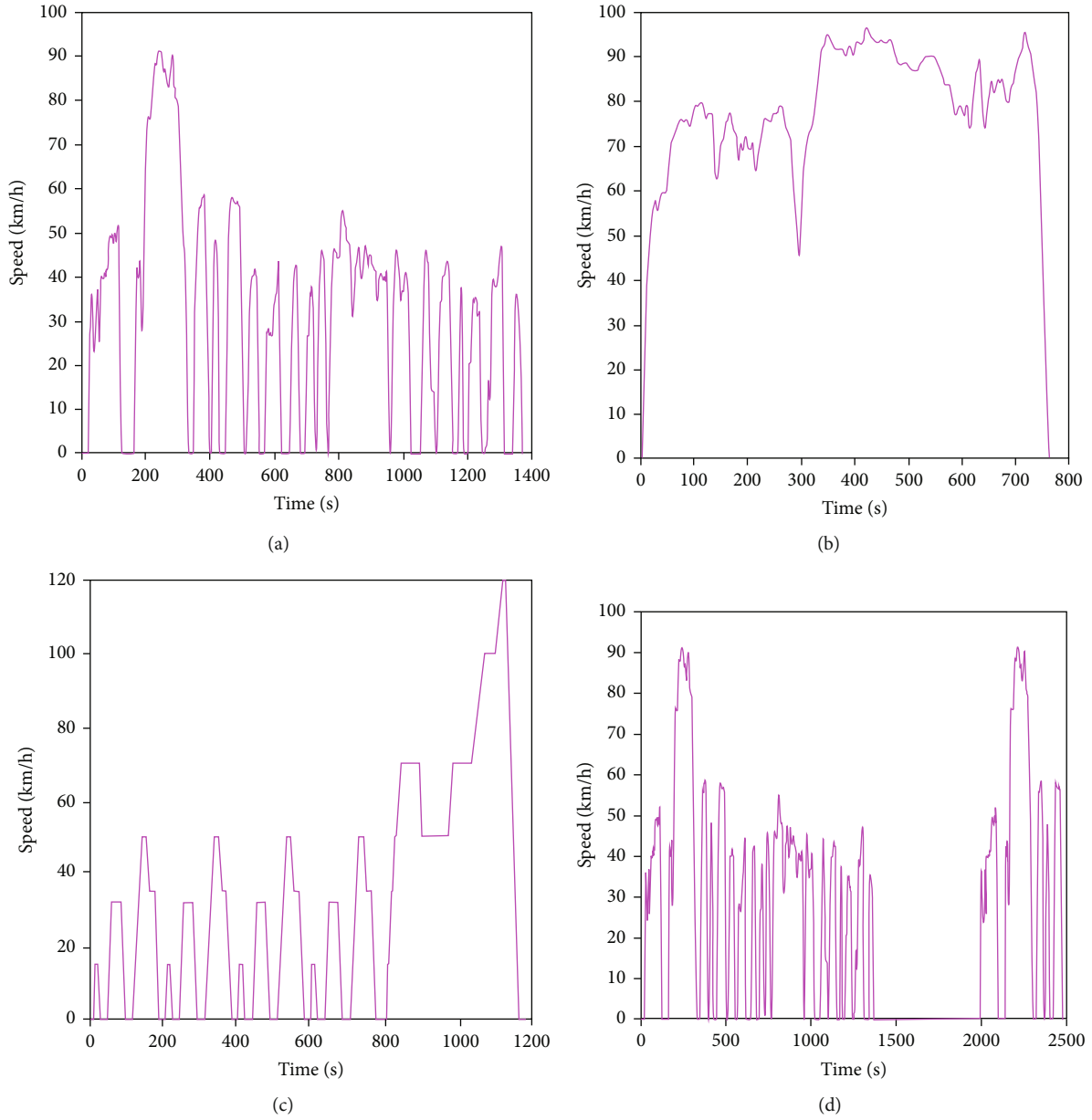
FIGURE 8: (a) UDDS, (b) HWFET, (c) NEDC, and (d) FTP driving cycle speed time graph.

consumed not only for power needs but also for thermal emissions and system losses.

In this configuration, the voltage of the fuel cell can drop because of losses that occur due to certain irreversibilities in the system. These losses are activation loss, ohmic loss, and concentration loss.

The activation loss is found by the Tafel equation. The Tafel equation represents the voltage drop on the surface as a result of the reaction of electrons with different electrochemical reactions. It is expressed by the following equation:

$$\Delta V_{act} = A \ln \left(\frac{i}{i_0} \right). \tag{1}$$

Here, $i_0 \left(A.cm^{-2} \right)$ represents the changing current density at the cathode, $i \left(A.cm^{-2} \right)$ represents the internal current density, and A represents the Tafel coefficient.

Membrane resistance is induced during the passage of electrons and protons, resulting in a voltage drop linearly dependent on the current. Ohmic loss is expressed by the following equation:

$$\Delta v_{ohm} = (R_{ele} + R_{mem})I = RI. \tag{2}$$

Here, $R_{ele} \left(\Omega cm^2 \right)$ represents the specific resistance of the electrodes, $R_{mem} \left(\Omega cm^2 \right)$ represents the specific resistance of the proton membrane, and $R \left(\Omega cm^2 \right)$ represents the total specific resistance.

The decrease in concentration causes a voltage drop. At large current densities, the voltage drop due to *concentration loss* is greater. This voltage drop is expressed by the following equation:

$$\Delta v_{\text{conc}} = c \ln \frac{i_L}{\dot{I}_L - i}. \tag{3}$$

Here, c is a constant representing the voltage drop due to loss of concentration, and $i_L (A.\text{cm}^{-2})$ represents limiting current density.

3.4. Fuel Cell Control Strategies. The power follower control system determines the torque and speed of the engine considering the conditions of the energy storage system, engine, and fuel cell. This strategy is used to minimize fuel usage and emissions. The main purpose of this control strategy is to add flexibility to the fuel cell system. The strategy aimed at low fuel consumption limits the output power of the fuel cell to certain ranges. As the fuel cell tends to follow the power needed by the power bus, the FC turns on if the power demanded by the power bus increases. It can be turned off again when the demanded power decreases, and the power and SOC of the energy storage system are sufficient.

3.5. Battery Model. The battery model is an equivalent circuit model consisting of an internal resistance and an open-circuit voltage source connected in series. The battery model consists of five submodels like the open circuit voltage and internal resistance model, power limiter, current calculation, charge state capacity, and thermal model. The battery model is shown in Figure 6.

Interpolated lookup tables are available for the open circuit voltage and the charge-discharge internal resistance values. Thanks to these parameters and lookup tables, the charge state capacity of the battery and thermal models can easily be created. Internal resistance and open circuit voltage values are scaled according to the number of modules in the battery series. The internal resistance is determined to be suitable for the charge and discharge cycles of the battery.

Meanwhile, the total power supplied by the battery is limited to the allowable ranges. Since the power demand is limited to zero, power cannot be drawn from a dead battery.

The state of charge (SOC) is an important parameter that shows the remaining energy of the battery and protects it from overcharging and discharging. SOC is calculated by the following equation:

$$\text{SOC} = \frac{\text{Remaining Charge (Ah)}}{\text{Capacity of the Battery (Ah)}}. \tag{4}$$

3.6. Supercapacitor Model. The supercapacitor circuit model is shown in Figure 7. The supercapacitor model consists of 4 submodels, which belong to supercapacitor voltage reading, calculation of current value, calculation of charge state capacity value, and thermal models.

This system limits the supercapacitor voltage according to its lower and upper limits. Supercapacitor voltage and SOC relationship are calculated as follows:

TABLE 1: Vehicle and energy storage system parameters.

	Parameter	Value
Vehicle	Vehicle mass (kg)	1191
	Wheel rolling radius (m)	0.282
	Wheelbase (m)	2.6
	Frontal area (m^2)	2
	Aerodynamic drag coefficient	0.335
	Coefficient of rolling drag	0.009
Electric motor/ controller	Motor type	AC induction
	Max power (kW)	75
	Maximum speed (rpm)	6283
	Total mass (kg)	91
	Average efficiency (%)	90
Fuel cell	Type	PEM fuel cell
	Total mass (kg)	223
	Max net power (kW)	50
	Average efficiency (%)	56
	Module number	25
Battery	Module mass (kg)	11
	Capacity (Ah)	25
	Rated voltage (V)	12
	Module number	155
Supercapacitor	Module mass (kg)	0.71
	Max voltage (V)	2.5
	Capacity (F)	2500

$$\text{SOC} = \frac{C * (V_{\text{OC}} - V_{\text{MIN}})}{C * (V_{\text{MAX}} - V_{\text{MIN}})} = \frac{V_{\text{OC}} - V_{\text{MIN}}}{V_{\text{MAX}} - V_{\text{MIN}}}. \tag{5}$$

Here, $C(F)$ represents the capacitor value, $V_{\text{OC}}(V)$ represents the open circuit voltage, and $V_{\text{MAX}}(V)$ and $V_{\text{MIN}}(V)$ represent the limited maximum and minimum voltage values.

The capacitor value is calculated as follows:

$$C = \frac{I * t}{V_W}, \tag{6}$$

where I (A) represents the current, t (s) is the time, and V_W (V) is the operating voltage.

3.7. Driving Cycles and Vehicle Parameters. UDDS driving cycle is short for Urban Dynamometer Driving Program. Used by the United States Environmental Protection Agency, it refers to the mandatory dynamometer test that represents city driving conditions for light vehicle testing on driving cycle fuel economy. The velocity-time graph of the cycle is shown in Figure 8(a). The driving cycle with a time of 1369 seconds represents a distance of 11.99 km. The driving cycle with an average speed of 31.51 km/h has 17 stops.

(a)

(b)

(c)

(d)
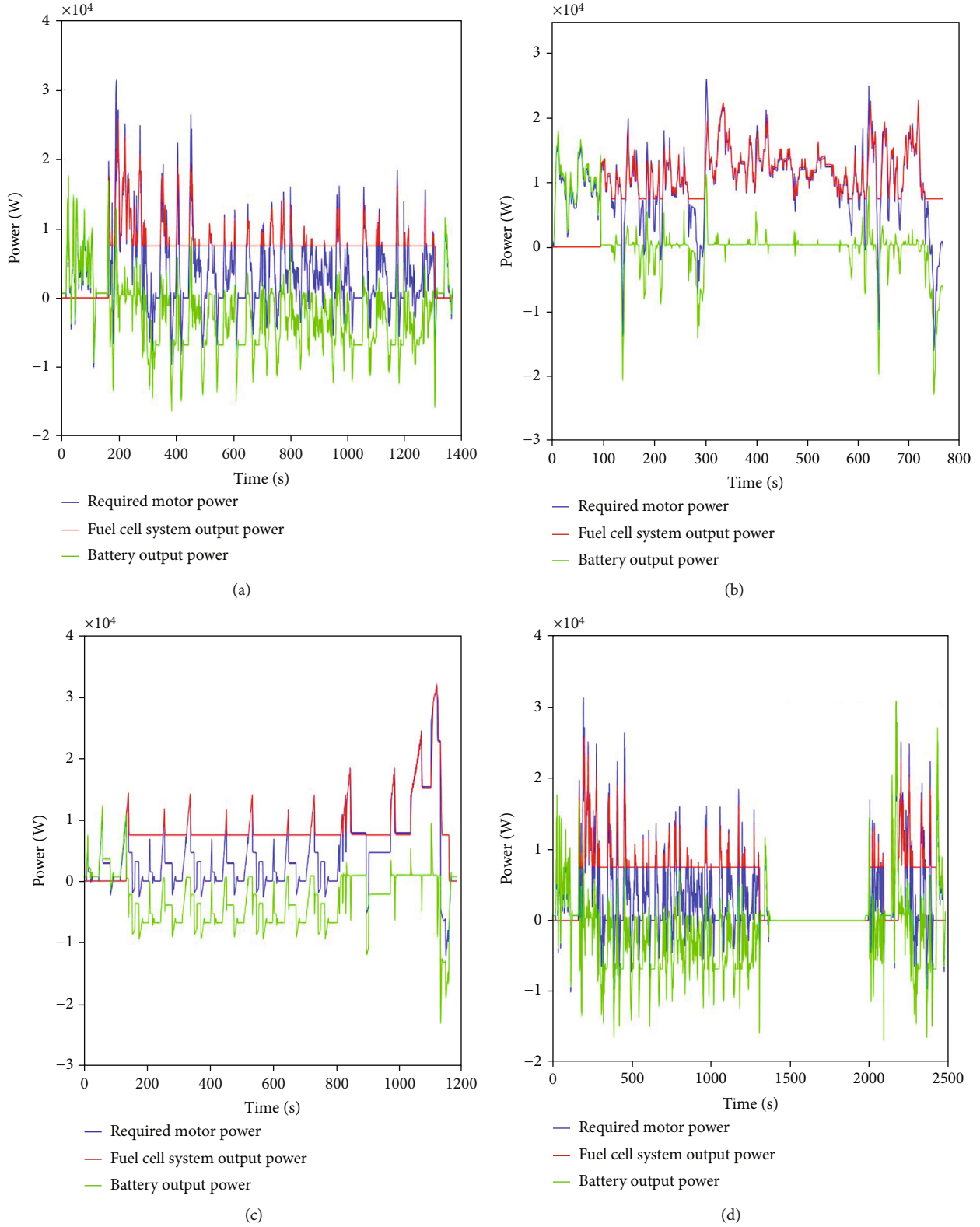
FIGURE 9: Power-time graph of (a) UDDS, (b) HWFET, (c) NEDC, and (d) FTP driving cycle of FC + B topology.

The Highway Fuel Economy Test (HWFET) cycle is the driving cycle developed by the US EPA for determining the fuel economy of light-duty vehicles. The velocity-time graph of the cycle is shown in Figure 8(b). The driving cycle with a time of 765 seconds consists of a distance of 16.51 km. The average speed of this driving cycle is 77.57 km/h, and it has only 1 stop.

(a)

(b)
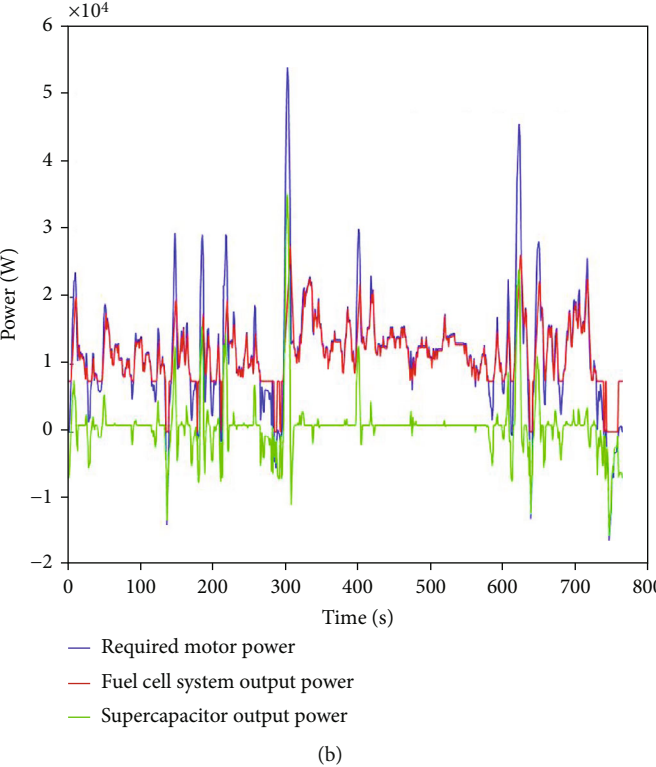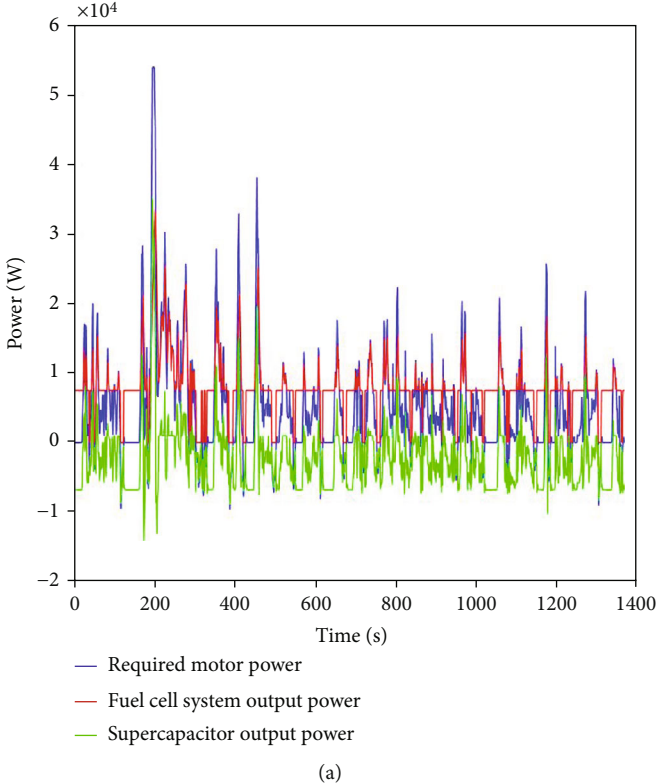
Figure 10: Continued.

(c)

(d)
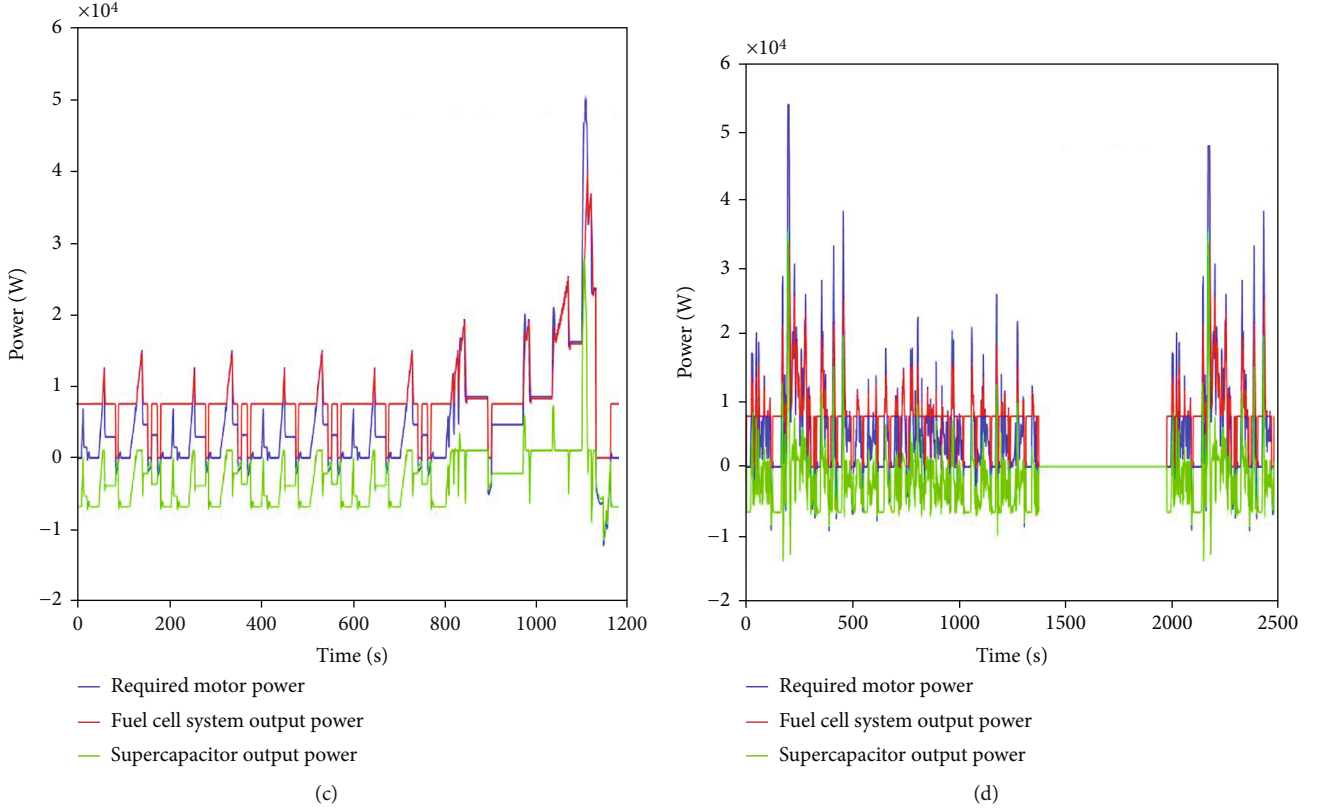
FIGURE 10: Power-time graph of (a) UDDS, (b) HWFET, (c) NEDC, and (d) FTP driving cycle of FC + SC topology.

The new European Driving Cycle (NEDC) is the driving cycle developed to measure emissions and fuel economy in cars. The velocity-time graph of the cycle is shown in Figure 8(c). The driving cycle with a time of 1184 seconds has a distance of 10.93 km. It has an average speed of 33.21 km/h, and it has 13 stops.

The Federal Test Procedure (FTP) used by the US Environmental Protection Agency is a set of tests defined to measure exhaust gas emissions and fuel economy of passenger vehicles for the urban driving cycle. The velocity-time graph of the cycle is shown in Figure 8(d). The driving cycle with a time of 2477 seconds has a distance of 17.77 km. It has an average speed of 91.25 km/h and 22 stops.

The vehicle and energy storage system parameters used in the modeling studies are shown in Table 1.

3.8. Energy and Exergy Analyses

3.8.1. Exergy Analysis. Although the first law of thermodynamics is mandatory to evaluate energy efficiency in the analyses, it does not give a complete conclusion about the potentials and usage limitations of the various components of an energy system analyzed by this law [26]. Instead, the first law of thermodynamics mainly deals with the amount of energy in a thermodynamic system. It is the second law of thermodynamics that deals with the performance and quality of the systems and gives better results about these aspects. Exergy analysis shows the maximum work potential of a given system by using the first and second laws together.

In this context, exergy is a measure of the system's potential to do work for a given environmental state [27]. Exergy analysis has gained great importance in the evaluation and design of systems. Exergy is lost, not conserved, due to the irreversibilities in the system. In light of these, a general exergy analysis reveals how much energy loss occurs in the system, as well as where it occurs [28].

Exergy, like energy, is broken down into its different components. Exergy E is expressed as in Equation (7) when electricity and surface tension, magnetism, and nuclear effects are ignored.

$$E = E_k + E_p + E_{phy} + E_{ch}. \tag{7}$$

Here, E_k represents kinetic exergy, E_p is the potential exergy, E_{phy} is the physical exergy, and E_{ch} chemical exergy. It is not included in the kinetic and potential exergy calculations.

Physical exergy is defined as the maximum work achieved by a substance at a given temperature and pressure in a stream, reaching the reference state by physical processes involving heat processes. Physical exergy is defined in Equation (8). Chemical exergy is due to the difference between the content of the current and the reference state [29].

$$E_{phy} = (H_1 - T_0 S_1) - H_0 - T_0 S_0, \tag{8}$$

$$E_{ch} = E_{ch}^0 + \sum (x \ln (x)). \tag{9}$$
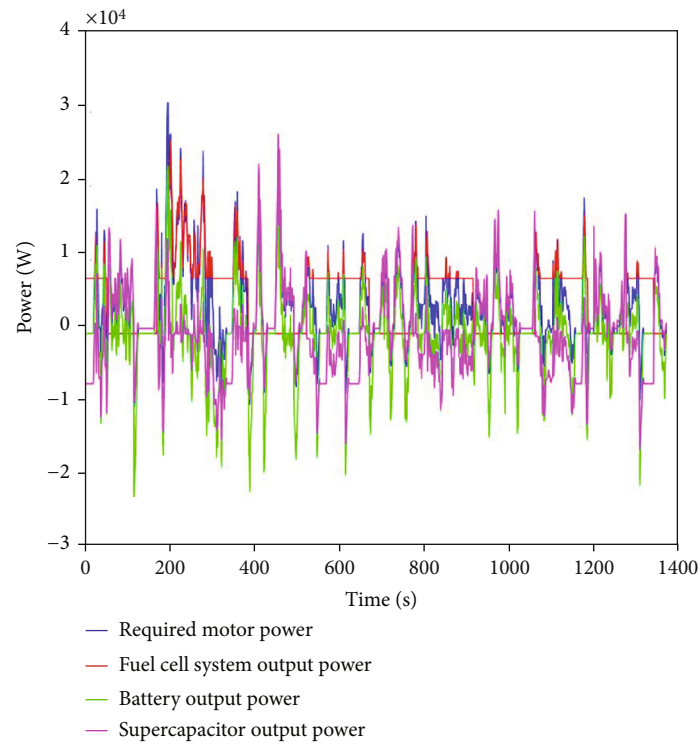
(a)
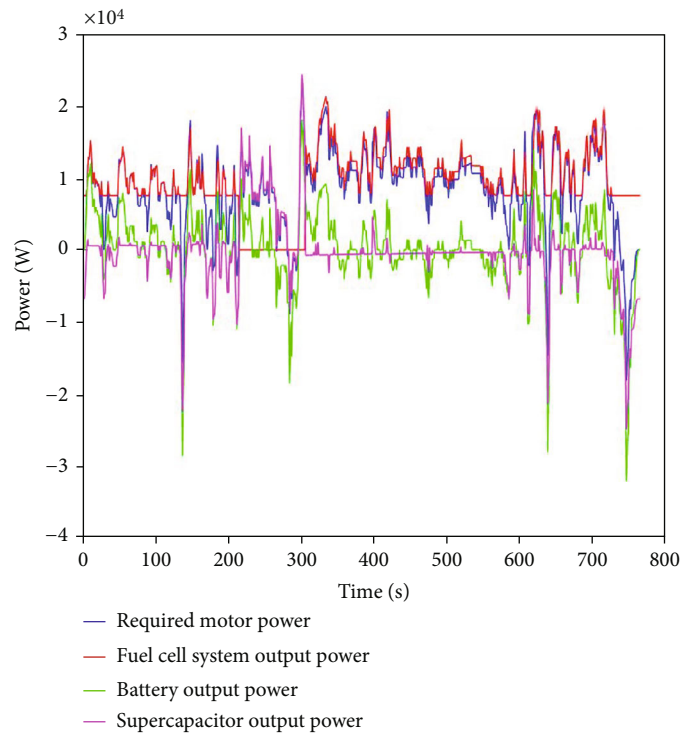
(b)

FIGURE 11: Continued.

(c)

(d)
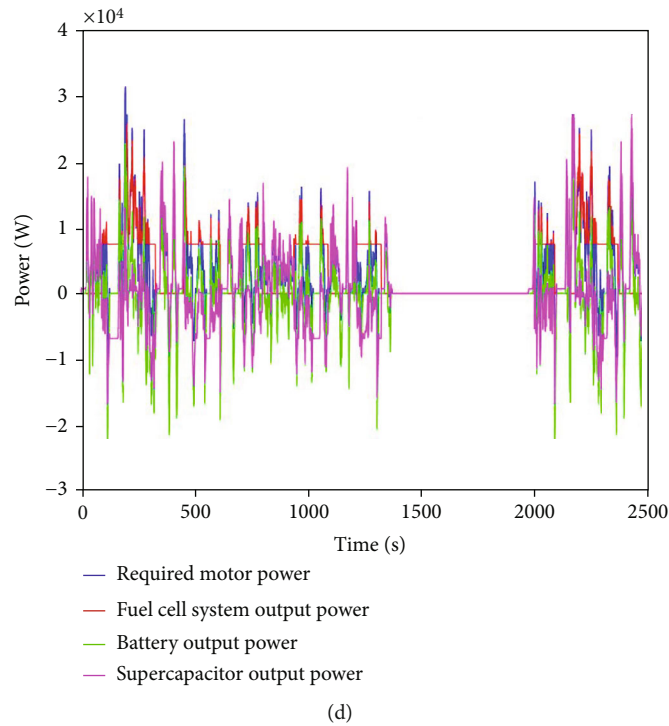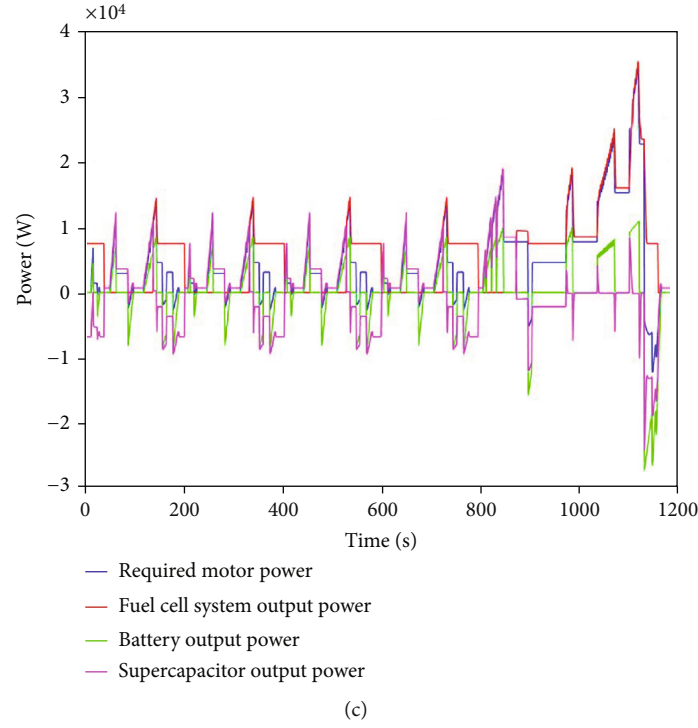
FIGURE 11: Power-time graph of (a) UDDS, (b) HWFET, (c) NEDC, and (d) FTP driving cycle of FC+ B + SC topology.

In Equations (8) and (9), H (J.mol^{-1}) represents enthalpy, S (J.mol^{-1}) represents entropy, T (K) represents temperature, and x represents mole fraction.

The exergy efficiency of the entire system in fuel cell vehicles was calculated by dividing the total aerodynamic force and rolling resistance by the total exergy. The calculation of exergy efficiency is shown in the following equation:

$$E_{\text{eff}} = \frac{\text{Aerodynamic Force (kJ)} + \text{Rolling Resistance(kJ)}}{\sum E \text{ (kJ)}} \times 100.$$

(10)

3.8.2. Energy Analysis. A fuel cell vehicle consists of a power bus, electric motor, gearbox, differential, wheels, and auxiliary

systems. The energy transferred from the hydrogen tank to the wheels loses energy according to the efficiency of each component on the path. Therefore, not all of the hydrogen energy can be transferred to the wheels. Some of the energy is transferred back to the energy storage system (battery, supercapacitor) by recovering some of it with regenerative braking which also affects the aerodynamic friction and rolling resistance. This affects the energy efficiency and performance of the entire system. The overall energy efficiency of the entire system realized at the end of the cycle is calculated by the following equation:

$$EN_{eff} = \frac{\text{Aerodynamic Force (kJ)} + \text{Rolling Resistance (kJ)}}{\text{Fuel in (kJ)} - \text{Energy Storage (kJ)}} \times 100. \tag{11}$$

4. Simulation Results

4.1. Fuel Cell + Battery Topology Results. FC/B, FC/SC, and FC/B/SC topologies were designed in the ADVISOR program in the Matlab/Simulink environment and applied in four different driving cycles and compared in terms of performance. Figure 9 shows the power-time graphs in the FC/B topology of the four driving cycles.

The durations vary according to the working times of the driving cycles. Here, the primary power source is the fuel cell. Looking at the power-time graphs, the battery provides the initial power required for starting and accelerating the vehicle, since it takes time to start the fuel cell. It has been observed that the fuel cell works at optimum points and sometimes works without load depending on the driving cycles. A large part of the vehicle's power demand is provided by the fuel cell, and in sudden and negative power demands, some of the power need is met by the battery. This energy is gained by the regenerative braking property of the system.

4.2. Fuel Cell + Supercapacitor Topology Results. In Figure 10, the power-time graphs in the FC + SC topology of the four driving cycles are shown.

It has been observed that the power demand in the FC/SC topology, the primary power source of which is the fuel cell, is mostly met by the fuel cell system. The varying power trends throughout the engine, fuel cell, and supercapacitor driving cycle coincide. Most of the instantaneous fluctuations are seen to be covered by the high power density supercapacitor. The supercapacitor plays an important role in providing extra power and can recover all the braking energy to provide temporary high power for the acceleration and climb phase.

4.3. Fuel Cell + Battery + Supercapacitor Topology Results. In Figure 11, the power-time graphs in the FC/B/SC topology of the four driving cycles are shown.

In this topology, the demand power of the motor is provided together by the FC system, the LIB package, and the supercapacitor. Due to the late commissioning of the fuel cell, the battery and supercapacitor provide the vehicle to start and accelerate in the first seconds. At the same time, battery and supercapacitor systems help to provide the power demanded by the driver by providing the necessary

Table 2: Performance summaries by driving cycles of all topologies.

Driving cycle	Fuel cell-based vehicle topology	Total hydrogen consumption (g)	Overall energy efficiency (%)	Overall exergy efficiency (%)
UDDS	FC + B	157.46	14.30	12.45
UDDS	FC + SC	174.10	11.00	11.20
UDDS	FC + B + SC	108.43	17.90	17.92
HWFET	FC + B	121.55	33.90	32.97
HWFET	FC + SC	136.70	31.50	31.90
HWFET	FC + B + SC	113.52	38.40	38.53
NEDC	FC + B	149.52	18.20	15.56
NEDC	FC + SC	157.98	14.50	14.69
NEDC	FC + B + SC	100.53	23.20	23.14
FTP	FC + B	204.71	16.70	15.28
FTP	FC + SC	243.09	12.70	12.79
FTP	FC + B + SC	150.97	19.90	19.82

energy in cases where the fuel cell is idle according to the driving cycles.

4.4. Hydrogen Consumption, Energy, and Exergy Analysis Results. The total hydrogen consumption, energy, and exergy efficiency percentages of the overall system in the UDDS, HWFET, NEDC, and FTP driving cycles of the FC + B, FC + SC, and FC + B + SC topologies are summarized in Table 2.

When the hydrogen consumption table of the three configurations is examined according to the four different driving cycles, it becomes apparent that the FTP driving cycle has the highest fuel consumption while the HWFET driving cycle has the least fuel consumption. This is because the FTP driving cycle has the highest distance at 17.77 km and the highest number of stops with 22 stops. The HWFET, on the other hand, has only 1 stop.

When the table examined in view of the three configurations, it is seen that the FC/B/SC topology has the least fuel consumption. The advantage of this topology is that the supercapacitor works at high power density, relieving the load of the battery and fuel cell, and at the same time, preventing continuous charging and discharging, thus prolonging their life. It helps the fuel cell to consume less fuel by not continuously charging and discharging. While FC/B and FC/B/SC have close fuel consumption values, FC/SC consumes more fuel compared to these two.

In the FC/B/SC topology, it has been observed that when the three powertrains work together, there is better energy and exergy efficiencies in all driving cycles. When the battery and supercapacitor state of charge is below the specified threshold, it helps to charge the energy storage system by operating the fuel cell at the maximum efficiency point. When the state of charge reaches the upper level, the fuel cell stops working. Therefore, the efficient use of the fuel cell in this topology has increased the energy and exergy efficiencies of the entire system.
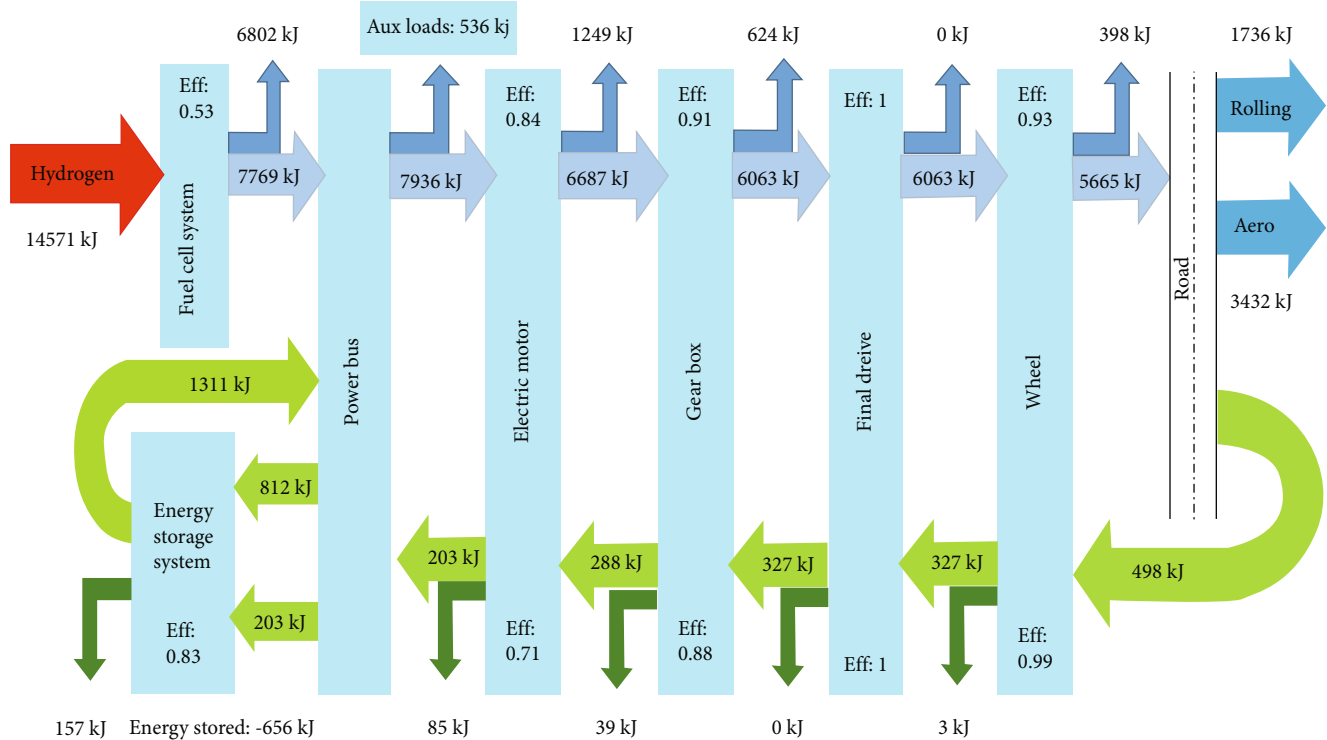
FIGURE 12: The energy flow of the vehicle system designed with HWFET drive in FC/B topology.

An energy flow diagram including the energy consumption and gains of the vehicle system designed with the HWFET drive in the FC/B topology is shown in Figure 12.

Figure 12 represents the energy flow from the hydrogen tank of the fuel cell vehicle to the wheels through the power bus, electric motor, gearbox, and the final drive. Arrows between components show energies transferred and lost from components. Since every component other than the power bus has energy loss, the initial energy from the hydrogen cannot be transferred directly to the wheels as a whole. At the same time, some of this energy is used for aerodynamic force and rolling resistance. Energy is transferred from the wheels to the energy storage system by regenerative braking. In this case, most of the energy loss occurs in the components. Since the fuel cell system alone has an efficiency of 53%, it is accepted to be more efficient when compared to conventional engines. 14571 kJ of energy is supplied to the fuel cell system from the hydrogen tank, and 5665 kJ of this energy can be transferred to the wheels. With regenerative braking, 498 kJ was transferred to the wheels, but only 203 kJ of this energy could be transferred to the energy storage system after component losses. While 1311 kJ of energy is transferred from the energy storage system to the vehicle components, at the end of the drive cycle, 656 kJ of energy has been removed from the storage system according to the initial charging state.

5. Conclusions

In this study, fuel cell + battery, fuel cell + supercapacitor, and fuel cell + battery + supercapacitor topologies are designed and modeled with the help of ADVISOR. Four dif-
ferent driving cycles UDDS, HWFET, NEDC, and FTP were applied to these topologies, and the fuel economy, energy efficiency, energy flow, exergy efficiency, and power analyses were made and compared according to the four driving cycles of the three topologies.

The power analysis shows that the battery helps the fuel cell to start and accelerate the vehicle in fuel cell + battery topologies, and it meets the power need thanks to regenerative braking, especially in sudden power demands. In the fuel cell + supercapacitor topology, it has been observed that the supercapacitor, thanks to its high power density, can meet the instantaneous fluctuations and transient high power. In the fuel cell + battery + supercapacitor topology, it has been determined that the battery and the supercapacitor work together to meet the power demand of the driver when the fuel cell is idle according to the driving cycle.

According to the hydrogen consumption results of the driving cycles, it has been observed that the FTP driving cycle is the most fuel-consuming since it has the highest distance at 17.77 km and the highest number of stops with 22 stops. The HWFET drive cycle with 1 stop was found to be the least fuel-consuming driving cycle. When the topologies are examined among themselves, it is seen that the FC/B/SC topology has the least fuel consumption, and the FC/SC topology consumes the most fuel. In the UDDS driving cycle, 9.557% less hydrogen consumption was achieved in FC/B and 37.72% less in FC/B/SC, respectively, compared to the FC/SC driving cycle. For the HWFET driving cycle, on the other hand, 11.082% and 16.96% less hydrogen were used in the FC/B and FC/B/SC topologies, respectively. In the NEDC driving cycle, 5.36% less fuel was used in the FC/B and 36.36% less in the FC/B/SC topology. Finally, in

the FTP driving cycle, there has been 15.79% and 37.90% lower hydrogen use in the FC/B and FC/B/SC topologies, respectively.

FC/B/SC topology has shown the best energy and exergy efficiencies in all four driving cycles. The highest energy and exergy efficiencies have been observed in the HWFET driving cycle. In this driving cycle, the FC/B/SC topology has 4.5% better energy efficiency than the FC/B topology and 6.9% better than the FC/SC driving cycle. At the same time, it is seen that FC/B/SC topology has 5.56% better exergy efficiency than FC/B topology and 6.63% better than FC/SC driving cycle.

The energy flow graph analysis of the HWFET drive cycle, which is one of the driving cycles with the best energy efficiency, was examined. The energy flow diagram from the fuel tank to the wheels and from the wheels to the energy storage system with regenerative braking is shown. The energy transferred according to the efficiency of each component affects the energy efficiency of the entire system. At the same time, the energy storage system in which the fuel cell operates at high efficiency and which supports the fuel cell with regenerative braking is also shown in this graphic.

Fuel cell-based hybrid vehicles are good environmentally friendly vehicle candidates with zero emissions and less fuel consumption. The production of FC/B topology models by leading car brands increases the interest and trust in FCEVs. The detailed study of fuel cell vehicle topologies and designs in the present study shows that FC/B/SC topology provides the best fuel consumption and the highest efficiency values amongst the candidate topologies.

Data Availability

No data was used for the research described in the article.

Conflicts of Interest

The authors declare that they have no conflicts of interest.

Acknowledgments

References

[1] D. D. Tran, M. Vafaeipour, M. El Baghdadi, R. Barrero, J. Van Mierlo, and O. Hegazy, "Thorough state-of-the-art analysis of electric and hybrid vehicle powertrains: Topologies and integrated energy management strategies," *Renewable and Sustainable Energy Reviews*, vol. 119, article 109596, 2020.

[2] T. E. Lipman, M. Elke, and J. Lidicker, "Hydrogen fuel cell electric vehicle performance and user-response assessment: Results of an extended driver study," *International Journal of Hydrogen Energy*, vol. 43, no. 27, pp. 12442–12454, 2018.

[3] L. Tribiolo, R. Cozzolino, and D. Chiappini, "Energy management of a plug-in fuel cell/battery hybrid vehicle with on-board fuel processing," *Applied Energy*, vol. 184, pp. 140–154, 2016.

[4] L. Xu, J. Li, M. Ouyang, J. Hua, and G. Yang, "Multi-mode control strategy for fuel cell electric vehicles regarding fuel economy and durability," *International Journal of Hydrogen Energy*, vol. 39, no. 5, pp. 2374–2389, 2014.

[5] J. Bauman and M. Kazerani, "A comparative study of fuel-cell–battery, fuel-cell–ultracapacitor, and fuel-cell–battery–ultracapacitor vehicles," *IEEE Transactions on Vehicular Technology*, vol. 57, no. 2, pp. 760–769, 2008.

[6] D. Feroldi, M. Serra, and J. Riera, "Design and analysis of fuel-cell hybrid systems oriented to automotive applications," *IEEE Transactions on Vehicular Technology*, vol. 58, no. 9, pp. 4720–4729, 2009.

[7] W. Gao, "Performance comparison of a fuel cell-battery hybrid powertrain and a fuel cell-ultracapacitor hybrid powertrain," *IEEE Transactions on Vehicular Technology*, vol. 54, no. 3, pp. 846–855, 2005.

[8] N. Sulaiman, M. A. Hannan, A. Mohamed, E. H. Majlan, and W. R. Wan Daud, "A review on energy management system for fuel cell hybrid electric vehicle: Issues and challenges," *Renewable and Sustainable Energy Reviews*, vol. 52, pp. 802–814, 2015.

[9] Ç. Bayindir, K. Gözüküçük, and A. Teke, "A comprehensive overview of hybrid electric vehicle: powertrain configurations, powertrain control techniques and electronic control units," *Energy Conversion and Management*, vol. 52, no. 2, pp. 1305–1313, 2011.

[10] W. Enang and C. Bannister, "Modelling and control of hybrid electric vehicles (a comprehensive review)," *Renewable and Sustainable Energy Reviews*, vol. 74, pp. 1210–1239, 2017.

[11] X. Hu, J. Jiang, B. Egardt, and D. Cao, "Advanced power-source integration in hybrid electric vehicles: multicriteria optimization approach," *IEEE Transactions on Industrial Electronics*, vol. 62, no. 12, pp. 7847–7858, 2015.

[12] S. Caux, Y. Gaoua, and P. Lopez, "A combinatorial optimisation approach to energy management strategy for a hybrid fuel cell vehicle," *Energy*, vol. 133, pp. 219–230, 2017.

[13] D. Fares, R. Chedid, F. Panik, S. Karaki, and R. Jabr, "Dynamic programming technique for optimizing fuel cell hybrid vehicles," *International Journal of Hydrogen Energy*, vol. 40, no. 24, pp. 7777–7790, 2015.

[14] B. S. Sami, N. Sihem, B. Zafar, and C. Adnane, "Performance study and efficiency improvement of Hybrid Electric System dedicated to transport application," *International Journal of Hydrogen Energy*, vol. 42, no. 17, pp. 12777–12789, 2017.

[15] A. Bathaee, "Multi-objective genetic optimization of the fuel cell hybrid vehicle supervisory system: fuzzy logic and operating mode control strategies," *International Journal of Hydrogen Energy*, vol. 40, no. 36, pp. 12512–12521, 2015.

[16] H. Aouzellag, K. Ghedamsi, and D. Aouzellag, "Energy management and fault tolerant control strategies for fuel cell/ultra- capacitor hybrid electric vehicles to enhance autonomy, efficiency and life time of the fuel cell system," *International Journal of Hydrogen Energy*, vol. 40, no. 22, pp. 7204–7213, 2015.

[17] I. Lachhab and L. Krichen, "An improved energy management strategy for FC/UC hybrid electric vehicles propelled by motor-wheels," *International Journal of Hydrogen Energy*, vol. 39, no. 1, pp. 571–581, 2014.

[18] Y. Zhou, A. Ravey, and M. C. Péra, "Multi-objective energy management for fuel cell electric vehicles using online-

learning enhanced Markov speed predictor," *Energy Conversion and Management*, vol. 213, p. 112821, 2020.

[19] Q. Li, W. Chen, Z. Liu, M. Li, and L. Ma, "Development of energy management system based on a power sharing strategy for a fuel cell-battery-supercapacitor hybrid tramway," *Journal of Power Sources*, vol. 279, pp. 267–280, 2015.

[20] Z. Chen, H. Hu, Y. Wu, Y. Zhang, G. Li, and Y. Liu, "Stochastic model predictive control for energy management of power-split plug- in hybrid electric vehicles based on reinforcement learning," *Energy*, vol. 211, p. 118931, 2020.

[21] J. Wu, N. Zhang, D. Tan, J. Chang, and W. Shi, "A robust online energy management strategy for fuel cell/battery hybrid electric vehicles," *International Journal of Hydrogen Energy*, vol. 45, no. 27, pp. 14093–14107, 2020.

[22] Y. Wang, Z. Sun, X. Li, X. Yang, and Z. Chen, "A comparative study of power allocation strategies used in fuel cell and ultracapacitor hybrid systems," *Energy*, vol. 189, article 116142, 2019.

[23] J. E. Valdez-Resendiz, J. C. Rosas-Caro, J. C. Mayo-Maldonado, A. Claudio-Sanchez, O. Ruiz-Martinez, and V. M. Sanchez, "Improvement of ultracapacitors-energy usage in fuel cell based hybrid electric vehicle," *International Journal of Hydrogen Energy*, vol. 45, no. 26, pp. 13746–13756, 2020.

[24] J. Alves, P. C. Baptista, G. A. Gonçalves, and G. O. Duarte, "Indirect methodologies to estimate energy use in vehicles: Application to battery electric vehicles," *Energy Conversion and Management*, vol. 124, pp. 116–129, 2016.

[25] T. Markel, A. Brooker, T. Hendricks et al., "ADVISOR: a systems analysis tool for advanced vehicle modeling," *Journal of Power Sources*, vol. 110, no. 2, pp. 255–266, 2002.

[26] L. Ozgener and A. Hepbaşli, "HVAC Sistemlerinde Ekserji Analizinin Gerekliliği Ve Uygulamaları," in *VI. Ulusal Tesisat Mühendisliği Kongresi ve Sergisi*, pp. 168-169, 2006.

[27] I. Dincer and M. A. Rosen, "Exergy and energy analyses," *Exergy*, pp. 23–35, 2021.

[28] A. Arshad, H. M. Ali, A. Habib, M. A. Bashir, M. Jabbal, and Y. Yan, "Energy and exergy analysis of fuel cells: a review," *Thermal Science and Engineering Progress*, vol. 9, pp. 308–321, 2019.

[29] S. O. Mert, I. Dincer, and Z. Ozcelik, "Performance investigation of a transportation PEM fuel cell system," *International Journal of Hydrogen Energy*, vol. 37, no. 1, pp. 623–633, 2012.